C. R. Mecanique 346 (2018) 603–614

Contents lists available at ScienceDirect

Comptes Rendus Mecanique

www.sciencedirect.com

Model reduction, data-based and advanced discretization in computational mechanics

Computing singular solutions to partial differential equations by Taylor series

Jie Yang [a,b], Heng Hu [a,*], Michel Potier-Ferry [b]

[a] School of Civil Engineering, Wuhan University, 8 South Road of East Lake, Wuchang, 430072 Wuhan, PR China
[b] Laboratoire d'étude des microstructures et de mécanique des matériaux, LEM3, UMR CNRS 7239, Université de Lorraine, île du Saulcy, 57045 Metz cedex 01, France

ARTICLE INFO

Article history:
Received 3 February 2018
Accepted 9 March 2018
Available online 27 April 2018

Keywords:
Taylor series
Meshless
Singular shape functions
Angular domain

ABSTRACT

The Taylor Meshless Method (TMM) is a true meshless integration-free numerical method for solving elliptic Partial Differential Equations (PDEs). The basic idea of this method is to use high-order polynomial shape functions that are approximated solutions to the PDE and are computed by the technique of Taylor series. Currently, this new method has proved robust and efficient, and it has the property of exponential convergence with the degree, when solving problems with smooth solutions. This exponential convergence is no longer obtained for problems involving cracks, corners or notches. On the basis of numerical tests, this paper establishes that the presence of a singularity leads to a worsened convergence of the Taylor series, but highly accurate solutions can be recovered by including a few singular solutions in the basis of shape functions.

1. Introduction

This paper deals with the numerical resolution of elliptic Partial Differential Equations (PDEs) by using Taylor series. The main interest of a Taylor series is the property of exponential convergence with the degree, which leads to strong reductions of the number of degrees of freedom (DOFs) as compared, for instance, with the finite element method [1,2]. Nevertheless the radius of convergence of a Taylor series is limited by the nearest singularity and singularities are common in engineering mechanics because of corners, cracks, or pointwise forces. So it is expected that such singularities will slow the convergence. In this paper, the relation between singular solutions and convergence of Taylor series is addressed.

Polynomial solutions to some PDEs have been used since a long time to build large finite elements, for instance in plane elasticity [3] or for plate bending [4], even with relatively large degrees. When associated with a specific treatment of boundary and interface conditions, this method has been called hybrid-Trefftz method, but there are also many other ways to account for these boundary-interfaces conditions [5]. Trefftz methods reduce dramatically the number of DOFs because only the boundary and interfaces have to be discretized, but it does not work as well for non-homogeneous and non-linear problems, in which cases exact solutions are not known. To extend the method into the non-linear range, it has been proposed to compute approximate solutions in the sense of Taylor series [6] and the latter procedure is efficient for a large class of PDEs, even in non-linear cases [7]. When coupled with appropriate collocation-based subdomain methods [2,8],

* Corresponding author.
E-mail address: huheng@whu.edu.cn (H. Hu).

https://doi.org/10.1016/j.crme.2018.04.003
1631-0721/

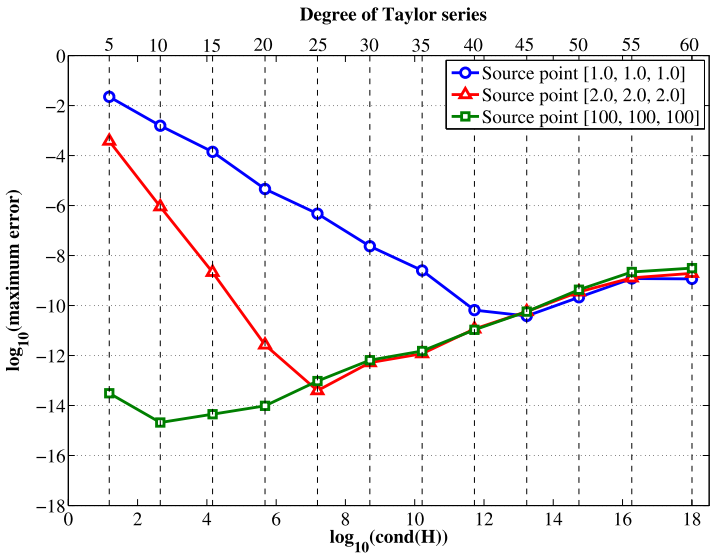

Fig. 1. Relative error versus conditioning for a degree varying from $p = 5$ up to $p = 60$. One tries to recover fundamental solutions within 3D linear elasticity. Three cases were considered. From [2].

it leads always to exponential convergence results. In this form, it has been called Taylor Meshless Method (TMM). These excellent convergence properties are illustrated in Fig. 1, where three problems are studied, one with a very flat response and two others with larger gradients. In the flat case, the convergence is very rapid and a small degree is sufficient to get a high precision ($\simeq 10^{-14}$) that is close to the limit for a real number in double-precision floating-point format. In the two other cases, there are two types of response. For a small degree, the response is governed by the exponential convergence of Taylor series, even for large domains. For larger degrees, the accuracy deteriorates slightly due to the propagation of round-off errors, which is favored by matrix ill-conditioning. The accuracy reversal observed in Fig. 1 is obtained for degrees $p = 25$ and $p = 45$, which means that TMM works well with large degrees. How to keep these excellent convergence properties when the solution is not analytic?

The treatment of singular solutions is a key issue in computational fracture mechanics. The bibliography on the topics is huge and we just refer, for instance, to [9] or [10]. Standard finite elements, which ignore the singular fields, could be used to analyze elastic cracked bodies, but this "should require extremely fine meshes" [9], so that various specific elements were introduced to better capture the singular behavior near the crack tip. The first one [11] simply consists in including the analytic singular functions and minimizing with respect to the stress intensity factors, but there are many variants in the literature of the seventies, see for instance [12] or [13]. The modern approaches, called extended finite element method or generalized finite element method, are based on the partition of unity [14] and can include analytic singular fields and discontinuities of the displacement [15]. Note that some problems with singular solutions were solved in a meshless framework by using a full basis of singular solutions [16,17].

The convergence properties of Taylor Meshless Method in the presence of singularities are addressed in this paper, especially for domains with corners and for classical crack problems. As expected, it is not possible to recover exponential convergence up to a high accuracy, in the same way as in Fig. 1. Building on the significant achievements within fracture mechanics, we shall combine the high-degree polynomials computed by Taylor series with analytically known singular solutions. Indeed the ability to solve problems with singular solutions is an important issue in the development of Taylor-based numerical methods.

2. Combining Taylor series and singular solution in a meshless framework

The issue of the present paper is the behavior of Taylor methods for elliptic systems having a singular solution. In this part 2, it will be shown that the convergence of Taylor methods, as illustrated in Fig. 1, deteriorates for corner-domains (Section 2.3). Next, a variant of the Taylor Meshless Method is proposed simply by including few singular solutions in the basis of shape functions (Section 2.4). For completeness, two main features of TMM are recalled: first the algorithm to compute polynomial approximate solutions to the PDE by the method of Taylor series (Section 2.1), next a procedure to build the global problem by a boundary least-square collocation method (Section 2.2).

2.1. Compute shape functions from Taylor series

The Taylor Meshless Method can be split in two parts. First the differential equation is solved in a quasi-exact manner by using the concept of Taylor series, next the boundary and interface conditions are accounted for by a collocation-based

technique. Let us begin by the solving inside the domain and describe the method for a simple two-dimensional linear PDE with mixed boundary conditions:

$$\begin{cases} -\Delta u(\boldsymbol{x}) + g(\boldsymbol{x})u(\boldsymbol{x}) = f(\boldsymbol{x}) & \boldsymbol{x} \in \Omega \\ u(\boldsymbol{x}) = u^d & \boldsymbol{x} \in \Gamma_d \\ \mathbf{T}u(\boldsymbol{x}) = t^n & \boldsymbol{x} \in \Gamma_n \end{cases} \tag{1}$$

where the function $u(\boldsymbol{x})$ is unknown, while $g(\boldsymbol{x})$ and $f(\boldsymbol{x})$ are given analytical functions, and $\mathbf{T}$ is a linear differential operator. Firstly, one expands $u(\boldsymbol{x})$, $g(\boldsymbol{x})$, and $f(\boldsymbol{x})$ by using truncated Taylor series with a development point $\boldsymbol{x}_c = [x_c, y_c]$. For convenience, the vector $\boldsymbol{x} - \boldsymbol{x}_c$ is denoted by $[\xi, \eta]$.

$$u(x, y) = \sum_{j=0}^{p} \sum_{i=0}^{j} \widetilde{u}(i, j-i) \xi^i \eta^{j-i} \tag{2}$$

$$g(x, y) = \sum_{j=0}^{p-2} \sum_{i=0}^{j} \widetilde{g}(i, j-i) \xi^i \eta^{j-i} \tag{3}$$

$$f(x, y) = \sum_{j=0}^{p-2} \sum_{i=0}^{j} \widetilde{f}(i, j-i) \xi^i \eta^{j-i} \tag{4}$$

where $\widetilde{u}(\,,\,)$, $\widetilde{g}(\,,\,)$ and $\widetilde{f}(\,,\,)$ represent the coefficients of the Taylor series of $u(\boldsymbol{x})$, $g(\boldsymbol{x})$ and $f(\boldsymbol{x})$, respectively. Note that only the coefficients $\widetilde{u}(\,,\,)$ are unknown.

The principle of the TMM is to vanish the residual $R(\boldsymbol{x})$ of the PDE up to the order $(p-2)$. Substituting Eqs. (2)–(4) into the PDE in Eq. (1), one can express $R(\boldsymbol{x})$ in the form of Taylor series:

$$\begin{aligned} R(\boldsymbol{x}) =& \Delta u(\boldsymbol{x}) - g(\boldsymbol{x})u(\boldsymbol{x}) + f(\boldsymbol{x}) \\ \approx& \sum_{m=0}^{p-2} \sum_{n=0}^{m} \widetilde{R}(m, n) \xi^m \eta^n \end{aligned} \tag{5}$$

where $\widetilde{R}(m, n)$ represents the coefficients of the Taylor series of the residual $R(\boldsymbol{x})$. The principle is to vanish these Taylor coefficients of the residual:

$$\begin{aligned} \widetilde{R}(m, n) =& (m+2)(m+1)\widetilde{u}(m+2, n) + (n+2)(n+1)\widetilde{u}(m, n+2) \\ & - \sum_{i=0}^{m} \sum_{j=0}^{n} \widetilde{g}(i, j)\widetilde{u}(m-i, n-j) + \widetilde{f}(m, n) = 0 \end{aligned} \tag{6}$$

The resulting equations can be considered as recurrence formulae permitting to compute a family of polynomials that are quasi-exact solutions to the PDE. In this way, one reduces the number of unknowns from $(p+1)(p+2)/2$ to $2p+1$. The latter independent unknowns are collected in a vector $\{\boldsymbol{v}\}$. Then the reduced expression u_p containing $2p+1$ unknowns writes:

$$\begin{aligned} u_p =& P_0(x, y, z) + \sum_{i=1}^{2p+1} P_i(x, y, z) v_i \\ =& P_0(x, y, z) + \langle \boldsymbol{P} \rangle \{\boldsymbol{v}\} \end{aligned} \tag{7}$$

where the first polynomial $P_0(x, y, z)$ balances the right-hand side $f(\boldsymbol{x})$ of Eq. (1), and $\langle \boldsymbol{P} \rangle$ collects the complete family of solutions to the associated homogeneous problems, see [2,6] for more details. As compared with Trefftz methods [5], the application to non-homogeneous and non-linear equations is straightforward.

2.2. Boundary least-square collocation

The polynomials P_0 and P_i in Eq. (7) are quasi-exact solutions to the PDE, in such a way that the discretization concerns only the boundary. As proposed in [6,18,19], a collocation technique combined with the least-square method can be used to account for boundary conditions. Two sets of nodes $\boldsymbol{x}_i$, $\boldsymbol{x}_j$ are chosen on Γ_d and Γ_n respectively (see Fig. 2). Then searching the variables $\{\boldsymbol{v}\}$ is equivalent to minimize the following function:

$$\mathscr{T}(\boldsymbol{v}) = \frac{1}{2} \sum_{\boldsymbol{x}_i \in \Gamma_d} \left| u_p(\boldsymbol{x}_i) - u^d(\boldsymbol{x}_i) \right|^2 + \omega \cdot \frac{1}{2} \sum_{\boldsymbol{x}_j \in \Gamma_n} \left| \mathbf{T}u_p(\boldsymbol{x}_j) - t^n(\boldsymbol{x}_j) \right|^2 \tag{8}$$

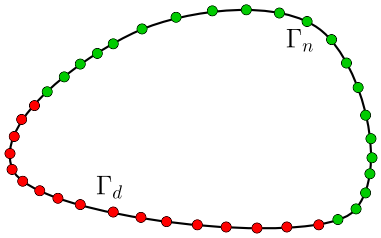

Fig. 2. Sketch for the boundary collocation method.

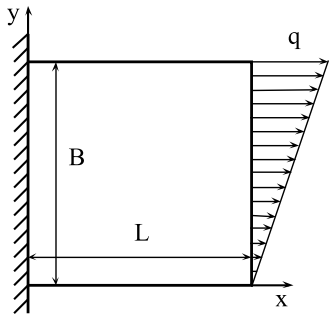

Fig. 3. A two-dimensional elasticity problem.

where ω permits to balance the two kinds of boundary conditions. In our tests, choosing different weight coefficients has little influence on the accuracy. Throughout this paper, the weight coefficient is set to be $\omega = 1$ for the numerical applications.

This minimization leads to a linear system $[\boldsymbol{K}]\{\boldsymbol{v}\} = \{\boldsymbol{b}\}$ where $[\boldsymbol{K}]$ is an invertible matrix. Solving this system gives the vector $\{\boldsymbol{v}\}$ and therefore the approximate solution to the problem of Eq. (1). The detailed expressions in the matrix $[\boldsymbol{K}]$ and the vector $\{\boldsymbol{b}\}$ write:

$$[\boldsymbol{K}]_{\alpha\beta} = \sum_{i=1}^{M_d} P_\alpha(\boldsymbol{x}_i) \cdot P_\beta(\boldsymbol{x}_i) + \omega \cdot \sum_{j=1}^{M_n} \mathbf{T}P_\alpha(\boldsymbol{x}_j) \cdot \mathbf{T}P_\beta(\boldsymbol{x}_j), \quad \alpha, \beta \in [1, 2p+1] \tag{9}$$

$$\{\boldsymbol{b}\}_\alpha = \sum_{i=1}^{M_d} P_\alpha(\boldsymbol{x}_i)(u^d(\boldsymbol{x}_i) - P_0(\boldsymbol{x}_i)) + \omega \cdot \sum_{j=1}^{M_n} \mathbf{T}P_\alpha(\boldsymbol{x}_j)(t^n(\boldsymbol{x}_j) - \mathbf{T}P_0(\boldsymbol{x}_j)) \tag{10}$$

where M_d and M_n represent the number of collocation points on the Dirichlet boundary Γ_d and the Neumann boundary Γ_n, respectively. This simple least-square collocation procedure will be applied in this paper, a single polynomial solution Eq. (7) being valid in the whole domain. Nevertheless, the same collocation method works well also to discretize interface conditions in a multi-domain approach [2] and alternative techniques are available for the discretization of the interface [8]. There are also finite element-based alternatives within the Trefftz community [3,5].

2.3. Convergence when the domain has a corner

What is the behavior of the latter method when the boundary is not smooth? Let us consider a problem of plane stress isotropic elasticity in a square domain with Dirichlet–Neumann boundary conditions as pictured in Fig. 3. The parameters are as follows: $L = B = 10$ mm, $E = 1000$ MPa (Young's modulus), $\nu = 0.3$ (Poisson's ratio) and $q = 100$ MPa. This problem has no analytical solution and we tried to define a reference solution by the finite element method. We consider that a 500×500 mesh with $Q4$ elements leads to a sort of reference solution. Indeed, with respect to a 250×250 mesh with $Q4$ elements or a 100×100 mesh with $Q8$ elements, the difference is less than $10^{-3.17}$. Throughout this paper, the effectiveness of the proposed technique will be evaluated by the maximum relative error between the approximated solution u_p and the reference solution u_{ref}, which is defined by:

$$\varepsilon = \frac{\max \left| u_p(\boldsymbol{x}) - u_{\text{ref}}(\boldsymbol{x}) \right|}{\max |u_{\text{ref}}(\boldsymbol{x})|} \tag{11}$$

This elasticity problem has been solved by the Taylor method presented in the previous sections. In this case, it was not possible to get a TMM-solution as accurate as in Fig. 1. The error decreases less quickly and there is a plateau of accuracy

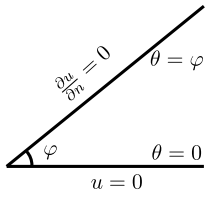

Fig. 4. Laplace equation in a circular sector with apex angle φ and Neumann–Dirichlet boundary conditions.

at about 1%, which is much larger than with problems having smooth solutions and larger than the difference between the two best FEM-results. More precisely, the maximal error is about 4% for a degree $p = 10$, 1.5% for $p = 30$ and only 1% for $p = 50$. Note also that the accuracy is better in the center of the domain ($\simeq 0.03\%$). Clearly, the worse convergence is due to the presence of the corners and this will be confirmed by forthcoming results.

2.4. A new TMM-procedure including singular shape functions

From the numerical test of Section 2.3, one sees the difficulty to recover the property of exponential convergence when the boundary is not smooth. To establish undoubtedly the connection between presence of corner and poor convergence, the Taylor series method of Sections 2.1 and 2.2 will be modified by including some singular shape functions. Indeed, it has been mathematically proved a long time ago [20,21] that the solution to an elliptic PDE in a domain with angular points can be split in two parts: a first part combining singular functions and a second part lying in a vectorial space of smoother functions. Thus it seems consistent to approximate this second part by a truncated Taylor series.

As it is well known, the family of singular solutions near a corner can be calculated analytically in many cases. For instance let us consider the Laplace equation $\Delta u = 0$ with Dirichlet–Neumann boundary conditions $u(r, 0) = 0$, $\frac{\partial u(r,\varphi)}{\partial \theta} = 0$, cf. Fig. 4. The general solution to $\Delta u = 0$ is in the form $u = \mathrm{Re}[\phi(z)]$, where $z = x + \mathrm{i}y = r\,\mathrm{e}^{\mathrm{i}\theta}$ and $\phi(z)$ is a holomorphic function. Hence, the singular solutions are in the form $\phi(z) = z^\alpha$ or $u(r, \theta) = r^\alpha \sin(\alpha\theta)$, taking into account the Dirichlet boundary condition (this solution is not smooth if α is not an integer). If one now introduces the Neumann boundary condition

$$\left.\frac{\partial u(r,\theta)}{\partial \theta}\right|_{\theta=\varphi} = \alpha r^\alpha \cos(\alpha\varphi) = 0, \tag{12}$$

one gets a countable family of possible exponents α:

$$\alpha_j \varphi = \frac{\pi}{2} + (j-1)\pi, \quad j = 1, 2, 3, \cdots \tag{13}$$

and the expressions of corresponding singular functions as follows

$$Q_j(r, \theta) = r^{\alpha_j} sin(\alpha_j \theta) \tag{14}$$

Such singular solutions can be built analytically for a number of PDEs, and we refer to Appendix A in the case of 2D elasticity. Next the simple way to take them into account is to combine linearly the non-singular solutions in Eq. (7) and the singular ones in Eq. (14). In the case of a homogeneous problem, this leads to the following ansatz:

$$u_{p,n}(\boldsymbol{x}) = \sum_{i=1}^{2p+1} v_i P_i(\boldsymbol{x}) + \sum_{j=1}^{n} v_{2p+1+j} Q_j(r, \theta) \tag{15}$$

Next we have to determine the $2p + 1 + n$ unknown coefficients v_i from the boundary conditions, what will be achieved by the same least-square collocation method described in Section 2.2. Transmission conditions could be accounted for in the same way in the case of multi-domain discretization, and there are alternative methods based on Lagrange multipliers [2,8]. Note that the coefficients $\{v_j, j \geq 2p + 2\}$ are often considered as quantities of interest. In fracture mechanics, the stress intensity factors belong to this set of coefficients.

3. Numerical applications

The modified Taylor method described in Section 2.4 is now analyzed by considering four numerical benchmarks related to the Laplace equation and 2D elasticity. Two of them have exact solutions, which permits to discuss the convergence up to a very high accuracy. These latter tests correspond to basic solutions in fracture mechanics. The two other cases are simple, but more generic, examples without exact solutions, which avoids some bias due to a too specific choice of the example. For these four simple cases, a multi-domain method is not necessary: the approximation in Eq. (15) holds in the whole domain.

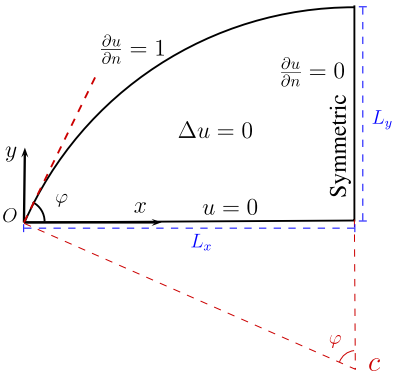

Fig. 5. Laplace equation in a circular segment. The solution is singular at the left corner.

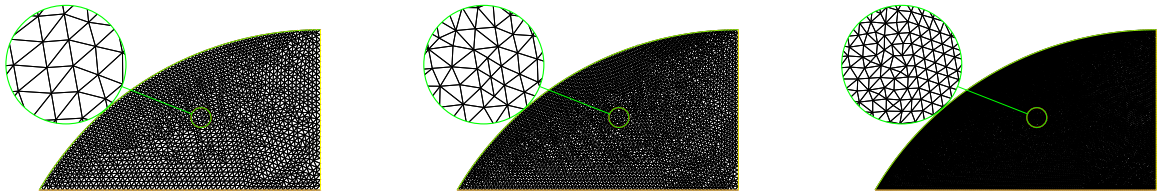

(a) Mesh one with 3810 elements (b) Mesh two with 6078 elements (c) Mesh three with 20576 elements

Fig. 6. Three meshes of the finite element models for the Laplace problem described in Fig. 5.

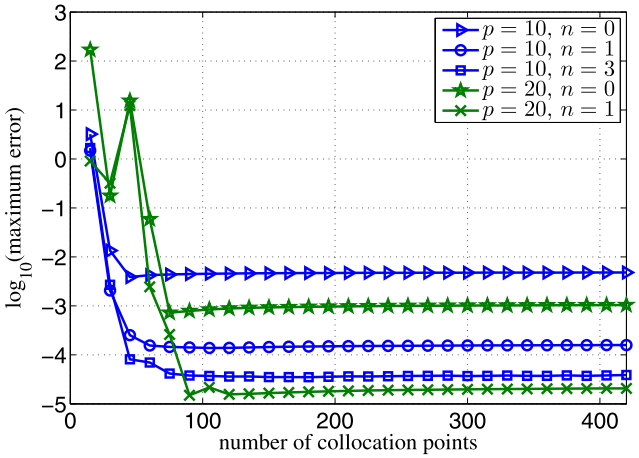

Fig. 7. The influence of the number of collocation points for the Laplace problem in Fig. 5, according to the degree p and the number n of singular shape functions.

3.1. Laplace equation with singularity

Here, we consider the Laplace equation in a domain that is a circular segment, as shown in Fig. 5. The left corner induces a rather weak singularity without infinite gradient at the corner ($\alpha_1 = 3/2$). The geometric parameters are as follows: $L_x = \sqrt{3}$, $L_y = 1$, $c = [\sqrt{3}, -1]$ and $\varphi = \pi/3$.

No analytical solution is available. A reference solution has been defined numerically by using the efficient open source code FreeFem++ [22]. Three different meshes with 6-node triangular elements were used as shown in Fig. 6. The finite element solution obtained by the most dense mesh (mesh three with 20576 P2 elements) is identified as a reference solution. Comparing mesh one (with 3810 P2 elements) and mesh two (with 6078 P2 elements) with mesh three respectively, one obtains an error equal to $10^{-4.7}$ and $10^{-4.62}$, respectively.

The optimal number of collocation points has been carefully discussed in previous papers [2,8]. Without singular functions, the number of degrees of freedom is $2p + 1$ in 2D and $(p + 1)^2$ in 3D and generally, the recommended number of collocation points is about the double. The influence of the number of collocation points is rediscussed here in the presence of singular shape functions, and this is illustrated in Fig. 7. It appears that the error remains always stable from a critical

Table 1
Convergence with the number of singular shape functions and the degree of non-singular polynomial shape functions for the Laplace problem defined in Fig. 5.

$\log_{10}(\varepsilon)$	$p=10$	$p=20$	$p=30$	$p=40$	$p=50$
$n=0$	−2.3498	−3.0184	−3.4256	−3.6733	−3.8487
$n=1$	−3.8493	−4.7543	−5.0174	−5.0227	−5.0246
$n=3$	−4.4218	−4.6921	−5.0171	−5.0225	−5.0217
$n=5$	−4.6823	−4.7546	−5.0174	−5.0221	−5.0196

number of collocation points, which is a little higher than $4(p+n)$. In the following, we choose $6(p+n)$ collocation points to ensure the convergence.

When enough collocation points are adopted, the accuracy is mainly dominated by the degree of polynomial shape functions p and the number of singular shape functions n. The convergence with p and n is presented in Table 1. Without singular shape functions ($n=0$), one converges slowly and reaches an accuracy of $10^{-3.8}$ for a large degree $p=50$. Just one or two singular shape functions permit to gain two orders of magnitude: for instance an accuracy of 10^{-4} require 101 DOFs without singular functions ($n=0, p=50$) while only 22 are sufficient with one singular shape function ($n=1, p=10$). Of course such results are consistent with the state of art within fracture mechanics [9] or with alternative results in a meshfree framework [16].

3.2. Two examples from linear elastic fracture mechanics

The two next examples are basic benchmarks of fracture mechanics. The behavior near a crack tip is more singular than in the example of Section 3.1, which means that the exponent α is smaller ($\alpha_1=\alpha_2=1/2$), and the stress is infinite at the crack tip ($\sigma\sim r^{-1/2}$). The two first coefficients in the singular part, called stress intensity factors (SIFs), are very important in fracture mechanics, and the accuracy with which these coefficients are obtained will be discussed. There is an ample literature about the computation of SIFs, but also of the full set of singular coefficients, see for instance [23]. In this paper, we are focused on the connection between singular shape functions and convergence of Taylor series, but the accuracy of the SIFs will be also shortly analyzed. Some information about the analytical calculation of the singular functions are recalled in Appendix A for completeness.

In this section, two fracture mechanics problems are considered. They are designed to have an analytical solution, which permits to measure very high accuracies. The solution to the first one is nothing but the famous mode I (or crack-opening mode) and it is one of the singular shape functions. As for the solution to the second problem, it comes from the problem of a cracked infinite plate under uniaxial tension. Note that the maximal error in Eq. (11) remains consistent for the displacement field that is continuous, but not for the stress that is not bounded at the crack tip. Nevertheless, this maximal error will be applied on a cloud of 50×50 points uniformly distributed on the domain except at the crack tip, where the control point has been moved of 0.001 (typically from $x=0.2$ to $x=0.201$).

3.2.1. A test to recover the crack opening model

The physical model is two-dimensional plane strain elasticity. The famous mode I of fracture mechanics corresponds to the following stress field:

$$\begin{cases}\sigma_x=\dfrac{K_{\mathrm{I}}}{\sqrt{2\pi r}}\cos(\theta/2)\cdot[1-\sin(\theta/2)\sin(3/2\cdot\theta)]\\ \sigma_y=\dfrac{K_{\mathrm{I}}}{\sqrt{2\pi r}}\cos(\theta/2)\cdot[1+\sin(\theta/2)\sin(3/2\cdot\theta)]\\ \tau_{xy}=\dfrac{K_{\mathrm{I}}}{\sqrt{2\pi r}}\cos(\theta/2)\cdot\sin(\theta/2)\cdot\cos(3/2\cdot\theta)\end{cases}\tag{16}$$

where $r=\sqrt{x^2+y^2}$, $\theta=\arctan(\frac{y}{x})$. The number K_{I} is the first stress intensity factor. The corresponding displacement field is:

$$\begin{cases}u=\dfrac{K_{\mathrm{I}}}{2\mu}(\dfrac{r}{2\pi})^{1/2}[\kappa-\cos(\theta)]\cos(\theta/2)\\ v=\dfrac{K_{\mathrm{I}}}{2\mu}(\dfrac{r}{2\pi})^{1/2}[\kappa-\cos(\theta)]\sin(\theta/2)\end{cases}\tag{17}$$

where $\kappa=3-4\nu$, ν is the Poisson ratio and $\mu=E/[2(1+\nu)]$. A mixed boundary value problem has been designed, see Fig. 8, whose solution is exactly given by Eqs. (16) and (17). The numerical value of the Poisson ratio is $\nu=0.3$ and the crack length is $a=0.2$ mm.

The Taylor method of Section 2.4 has been applied to this problem, without and with singular shape functions. As expected, it is not possible to get accurate solutions without singular solutions, the errors in displacement being always

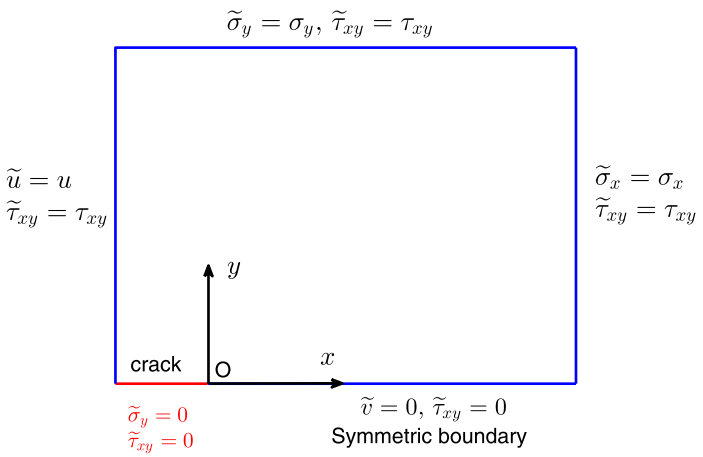

Fig. 8. A boundary value problem to recover the crack opening mode.

Table 2
Convergence with the degree p and the number of singular functions n for the mode I problem described in Fig. 8.

n	p	NDOFs	Error in displacement $\log_{10}(\varepsilon)$	Error in stress $\log_{10}(\varepsilon)$
$n=2$	1	8	−15.1204	−15.2682
	10	44	−12.8060	−12.6139
	20	84	−11.2045	−10.1424
$n=6$	1	12	−15.1804	−15.3474
	10	48	−12.5630	−12.2353
	20	88	−10.8113	−10.0309

larger than 50%, even for large degrees $p=30$ and $p=50$: hence, it seems difficult to use only polynomial shape functions to recover a singular solution. Some results with singular shape functions are presented in Table 2. When two singular shape functions ($\alpha_1=\alpha_2=1/2$) and three polynomial shape functions (i.e. a degree $p=1$) are used, the maximum relative errors on displacements and stresses are very small: $10^{-15.1}$ and $10^{-15.3}$, respectively. Such an error is very close to the unit round-off error $2^{-52}\approx 2.22\times 10^{-16}$ for a single real number within the double-precision floating-point format [24,25]. If one increases the degree, the accuracy deteriorates slightly, because of the propagation of round-off errors. The same very specific scheme was also observed if one tries to get a polynomial solution by the pure Taylor method of Section 2.1. This behavior is typical of problems where the exact solution lies in the vectorial space generated by the shape functions [2].

3.2.2. The infinite plate with a central crack under tensile stress

The second fracture benchmark emanates from the problem of an infinite medium with a horizontal central crack of length $2a$ and submitted to a uniaxial stress $\sigma^\infty \mathbf{e}_y\otimes\mathbf{e}_y$ at infinity, see Fig. 9a. The analytical solution is well known [26,27]:

$$\begin{cases} u = \frac{\sigma^\infty}{2\mu}\left[\frac{(\kappa-1)}{2}(r_2^{1/2}\cos(\theta_2/2) - \frac{1}{2}r_1\cos(\theta_1)) - y\cdot r_1\cdot r_2^{-1/2}\sin(\theta_1+\theta_2/2) - \frac{x}{2}\right] \\ v = \frac{\sigma^\infty}{2\mu}\left[\frac{-(\kappa+1)}{2}(r_2^{1/2}\sin(\theta_2/2) + \frac{1}{2}r_1\sin(\theta_1)) - y\cdot r_1\cdot r_2^{-1/2}\cos(\theta_1+\theta_2/2) + y\right] \end{cases} \tag{18}$$

$$\begin{cases} \sigma_x = \sigma^\infty\cdot r_1\cdot r_2^{-1/2}\left[\cos(\theta_1+\theta_2/2) + a^2\cdot r_2{}^{-1}\cdot\sin(\theta_1)\sin(3/2\cdot\theta_2)\right] - \sigma^\infty \\ \sigma_y = \sigma^\infty\cdot r_1\cdot r_2^{-1/2}\left[\cos(\theta_1+\theta_2/2) - a^2\cdot r_2{}^{-1}\cdot\sin(\theta_1)\sin(3/2\cdot\theta_2)\right] \\ \tau_{xy} = \sigma^\infty\cdot a^2\cdot r_1\cdot r_2^{-1/2}\cdot\sin(\theta_1)\cdot\cos(3/2\cdot\theta_2) \end{cases} \tag{19}$$

where the r_1, θ_1 and r_2, θ_2 are defined as follows:

$$\begin{cases} r_1 = \sqrt{x^2+y^2}; & \theta_1 = \arctan(\dfrac{y}{x}). \\ r_2 = \sqrt{(x^2-y^2-a^2)^2+(-2xy)^2}; & \theta_2 = \arctan(\dfrac{-2xy}{x^2-y^2-a^2}) \end{cases} \tag{20}$$

The chosen parameters are as follows: $a=0.2$ mm, $\sigma^\infty=100$ MPa, $\nu=0.3$, $\kappa=3-4\nu$, $E=1000$ MPa (Young's modulus), and $\mu=E/[2(1+\nu)]$. A square domain has been cut in the infinite domain (see Fig. 9a), and a corresponding boundary value problem has been posed in Fig. 9b so as to keep the same solution, Eqs. (18) and (19).

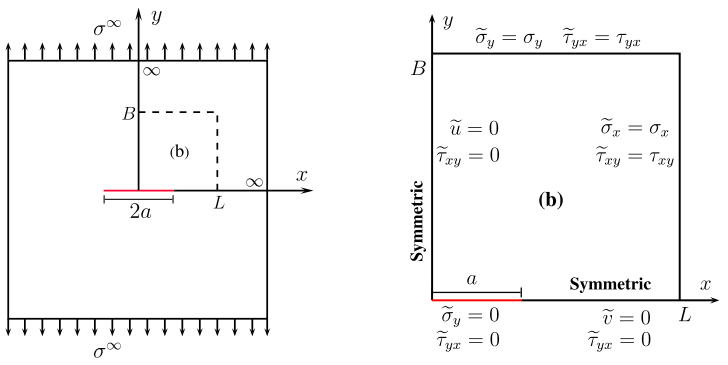

Fig. 9. (a) The infinite plate with a central crack and submitted to a uniaxial stress at infinity; (b) A boundary value problem in a finite domain whose solution is the same as for the infinite plate of Fig. 9a.

Table 3
Convergence with the degree p and the number of singular functions n for the cracked plate problem described in Fig. 10.

n	p	Error in displacements $\log_{10}(\varepsilon)$	Error in stresses $\log_{10}(\varepsilon)$	Error in SIFs $\log_{10}(\varepsilon)$
$n=2$	10	−1.4137	−1.3121	−1.5543
	30	−2.0785	−1.6041	−1.5914
	50	−2.2081	−1.5592	−1.7093
$n=6$	10	−2.3236	−1.6326	−2.5541
	30	−4.7309	−4.2851	−4.4160
	50	−5.8604	−5.1474	−5.0110
$n=8$	10	−2.4972	−1.7541	−2.4210
	30	−5.0535	−4.5884	−5.8802
	40	−6.2975	−5.6968	−6.0031
	50	−5.6359	−4.8222	−5.8995

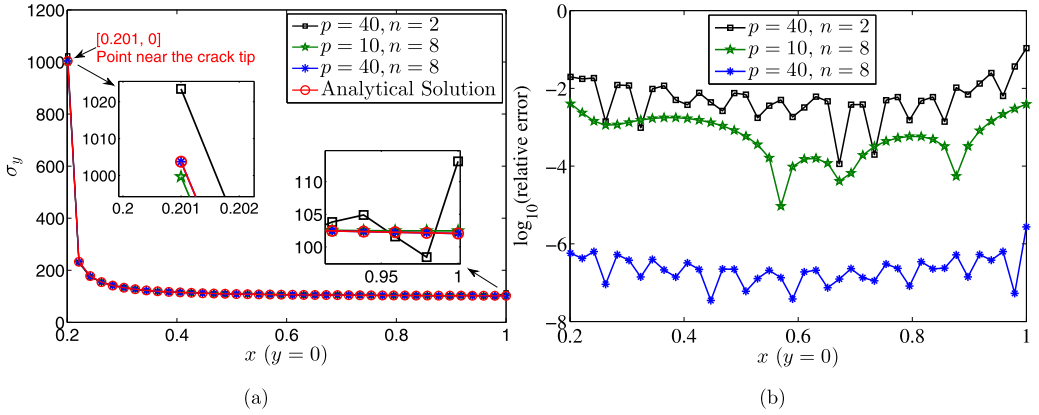

Fig. 10. The distribution of transverse stress σ_y and of the corresponding error along the horizontal line $y = 0$.

The convergence with the degree p of the polynomial shape functions and the number n of singular shape functions is now discussed. The numerical solution is wrong without singular shape functions, the error being at least 50%. Table 3 presents the obtained accuracy from two to eight singular functions. The introduction of two singular functions is sufficient to get an error of about 1%. Next the accuracy is easily improved by increasing the number of singular functions and the degree. For instance, with a degree $p = 10$ (42 polynomials), one passes from an error of $10^{-1.4}$ for $n = 2$ to an error of $10^{-2.3}$ for $n = 6$, and finally to $10^{-3.3}$ for $n = 20$. There is a plateau of accuracy at a high level (10^{-5} or 10^{-6}). Moreover, the error in stress and Stress Intensity Factor has about the same order of magnitude as for the displacement. The convergence with these two parameters p and n is also illustrated in Fig. 10, where the distribution of transverse stress σ_y is plotted: one sees clearly the strong improvement obtained by increasing the number of singular functions from $n = 2$ to $n = 8$.

Table 4
Convergence with degree in the presence of few singular functions for the square elasticity shown in Fig. 3.

n	p	Error of v ($\log_{10}(\varepsilon)$)
$n_1 = n_2 = 1$	10	−2.4695
	30	−3.4594
	50	−3.5111
$n_1 = n_2 = 2$	10	−2.5001
	30	−3.4637
	50	−3.6689

3.3. Application in two-dimensional elasticity

Let us come back to the 2D elasticity problem of Fig. 3. The accuracy of TMM without singular functions was not better than 1%. The accuracy of the vertical displacement v with two and four singular functions is reported in Table 4. Two types of singular functions are used: n_1 and n_2 singular functions located at upper-left and bottom-left corners respectively. At least one order of magnitude is gained simply by adding one singular function at each corner ($n_1 = n_2 = 1$), the error being reduced to 0.035% for a degree $p = 30$ and for $n_1 = n_2 = 1$. This establishes once more the connection between singularities and bad convergence of Taylor series, as well as a simple manner to get tremendous improvements of this convergence. Note that the maximal error mentioned in the Table ($10^{3.67}$) may be due as well to FEM as to TMM.

4. Conclusion

A boundary collocation meshless method involving high-order polynomial shape functions and singular shape functions was proposed in this paper to solve problems with singularities. Since these shape functions are the approximated solutions to the considered problems, discretization concerns only the boundary, and least-square collocation is employed to determine the unknown coefficients. Based on previous research, the proposed technique without singular shape functions always works well when the solution to a considered problem is smooth, while it fails to recover the solution of problem with singularities. So we wonder what is the probability of solving singular problem effectively by introducing singular shape functions. It was well established [20] that the solution to a problem in an angular domain can be split in a smooth part and a linear combination of singular functions: in the present method, the smooth part is discretized by Taylor series.

Few benchmark tests established that the accuracy of the approximated solution is widely improved by introducing few singular shape functions. When enough collocation points are chosen, accuracy is dominated by two factors: the degree of polynomial shape functions and the number of singular shape functions. For a fixed number of singular shape functions, the proposed technique converges with the degree of polynomial shape functions. And for a fixed degree of polynomial shape functions, accuracy increases with the number of singular shape functions.

Acknowledgements

This paper is dedicated to Pierre Villon, who is the author of many prominent contributions in computational mechanics. Michel Potier-Ferry is particularly grateful to Pierre for many helpful discussions about meshfree methods. This work has been supported by the National Natural Science Foundation of China (Grant No. 11372231). The authors acknowledge the financial support of the Chinese–French program Cai Yuanpei (China Scholarship Council)/Hubert Curien (PROJECT No. 32107UB). Michel Potier-Ferry acknowledges also the French National Research Agency ANR (Labex DAMAS, Grant ANR-11-LABX-0008-01).

Appendix A. Singular solutions to opening crack

In this Appendix, we compute analytically the whole set of singular functions in the case of a crack tip. This is based on the well-known complex variable method, and we refer the reader to [27] for the details. A similar approach can be done for the square domain problem in Fig. 3.

The Airy stress function U satisfying the biharmonic equation $\Delta^2 U = 0$ reads:

$$U = \mathrm{Re}\left[\overline{z}\varphi(z) + \chi(z)\right] \tag{21}$$

where $z = x + \mathrm{i}y$ and both $\varphi(z)$ and $\chi(z)$ are harmonic functions.

The complex representation of displacements denotes

$$2\mu(u + \mathrm{i}v) = \kappa\varphi(z) - z\overline{\varphi'(z)} - \overline{\chi'(z)} \tag{22}$$

where ν and μ represent the Poisson's ratio and the shear modulus, respectively. The number κ is a constant related to ν and it takes the value $3 - 4\nu$ for plane strain, while it takes the value $(3 - \nu)/(1 + \nu)$ for generalized plane stress. The complex representations of stresses denote

$$\begin{cases} \sigma_x + \sigma_y = 2\left[\varphi'(z) + \overline{\varphi'(z)}\right] \\ \sigma_y - \sigma_x + 2\mathrm{i}\tau_{xy} = 2\left[\overline{z}\varphi''(z) + \psi'(z)\right] \end{cases} \tag{23}$$

The force acting on an arc AB then can be expressed by:

$$X + \mathrm{i}Y = -\mathrm{i}\left[\varphi(z) + z\overline{\varphi'(z)} + \overline{\psi(z)}\right]_{\mathrm{A}}^{\mathrm{B}} \tag{24}$$

where $\psi(z) = \chi'(z)$.

One sets the harmonic functions as follows: $\varphi(z) = c_1 z^{\alpha}$ and $\psi(z) = c_2 z^{\alpha}$, where α is a real number and c_1, c_2 are unknown complex numbers determined by the boundary conditions on the upper and lower surfaces of the crack tip. The force $(X + \mathrm{i}Y)$ vanishes along the crack tip, hence the Eq. (24) satisfies the following conditions:

$$\varphi(z) + z\overline{\varphi'(z)} + \overline{\psi(z)} = 0, \quad \theta = \pm\pi \tag{25}$$

The following relationships can be obtained from Eq. (25):

$$\begin{cases} c_1 \mathrm{e}^{\mathrm{i}\alpha\pi} + \overline{c_1}\alpha\mathrm{e}^{-\mathrm{i}\alpha\pi} + \overline{c_2}\alpha\mathrm{e}^{-\mathrm{i}\alpha\pi} = 0 \\ c_1 \mathrm{e}^{-\mathrm{i}\alpha\pi} + \overline{c_1}\alpha\mathrm{e}^{\mathrm{i}\alpha\pi} + \overline{c_2}\alpha\mathrm{e}^{\mathrm{i}\alpha\pi} = 0 \end{cases} \tag{26}$$

Considering Eq. (26), one can get

$$\mathrm{e}^{\mathrm{i}\cdot 4\alpha\pi} = 1 \tag{27}$$

which means $\alpha = \frac{1}{2}, 1, \frac{3}{2}, 2, \frac{5}{2}, \cdots$. To ensure the singularity of the approximation, the integer values of α should be removed. Finally, $\alpha = \frac{1}{2}, \frac{3}{2}, \frac{5}{2}, \cdots$ are obtained.

Considering the value of α deduced from the boundary conditions, one can get the following relationship between c_1 and c_2 by Eq. (26):

$$c_2 = -c_1\alpha + \overline{c_1} \tag{28}$$

If c_1 is set to be 1 and i respectively, these corresponding values of c_2 are as follows:

$$\begin{cases} c_1 = 1, \quad c_2 = 1 - \alpha \\ c_1 = i, \quad c_2 = -i(1 + \alpha) \end{cases} \tag{29}$$

Substituting the values of c_1 and c_2 in Eqs. (22) and (23), one can obtain the expressions of displacements and stresses as follows:

- the first set of singular solutions, $c_1 = 1$ and $c_2 = 1 - \alpha$:

$$\begin{cases} u = \frac{1}{2\mu} r^{\alpha} \left[(\kappa - 1 + \alpha) \cdot \cos(\alpha\theta) - \alpha \cdot cos\left((2 - \alpha)\theta\right)\right] \\ v = \frac{1}{2\mu} r^{\alpha} \left[(\kappa + 1 - \alpha) \cdot \sin(\alpha\theta) - \alpha \cdot sin\left((2 - \alpha)\theta\right)\right] \end{cases} \tag{30}$$

$$\begin{cases} \sigma_x = r^{\alpha-1} \cdot \alpha \cdot [(\alpha + 1)\cos((\alpha - 1)\theta) - (\alpha - 1)\cos((\alpha - 3)\theta)] \\ \sigma_y = r^{\alpha-1} \cdot \alpha \cdot [(3 - \alpha)\cos((\alpha - 1)\theta) + (\alpha - 1)\cos((\alpha - 3)\theta)] \\ \tau_{xy} = r^{\alpha-1} \cdot \alpha \cdot (\alpha - 1)\left[\sin((\alpha - 3)\theta) - \sin((\alpha - 1)\theta)\right] \end{cases} \tag{31}$$

- The second set of singular solutions, $c_1 = \mathrm{i}$ and $c_2 = -\mathrm{i}(1 + \alpha)$:

$$\begin{cases} u = \frac{-1}{2\mu} r^{\alpha} \left[(\kappa + 1 + \alpha) \cdot \sin(\alpha\theta) + \alpha \cdot sin\left((2 - \alpha)\theta\right)\right] \\ v = \frac{1}{2\mu} r^{\alpha} \left[(\kappa - 1 - \alpha) \cdot \cos(\alpha\theta) + \alpha \cdot cos\left((2 - \alpha)\theta\right)\right] \end{cases} \tag{32}$$

$$\begin{cases} \sigma_x = r^{\alpha-1} \cdot \alpha \cdot [(\alpha - 1)\sin((\alpha - 3)\theta) - (\alpha + 3)\cos((\alpha - 1)\theta)] \\ \sigma_y = r^{\alpha-1} \cdot \alpha \cdot (\alpha - 1)\left[\sin((\alpha - 1)\theta) - \sin((\alpha - 3)\theta)\right] \\ \tau_{xy} = r^{\alpha-1} \cdot \alpha \cdot [(\alpha - 1)\cos((\alpha - 3)\theta) - (\alpha + 1)\sin((\alpha - 1)\theta)] \end{cases} \tag{33}$$

Selecting one value of α, there will be two sets of singular solutions. The way to deduce the non-singular shape functions from Taylor series has been introduced in section 2.1. The linear combination of the non-singular shape functions and singular solutions shown in Eqs. (30) and (32) leads to the approximations of this considered problem. Since the approximations satisfy the control equations, only boundary conditions need to be considered to determine the unknown coefficients. This last step is realized by using the least-square collocation technique as shown in section 2.2.

References

[1] Y. Tampango, M. Potier-Ferry, Y. Koutsawa, S. Belouettar, Convergence analysis and detection of singularities within a boundary meshless method based on Taylor series, Eng. Anal. Bound. Elem. 36 (10) (2012) 1465–1472.
[2] J. Yang, H. Hu, M. Potier-Ferry, Solving large scale problems by Taylor Meshless Method, Int. J. Numer. Methods Eng. 112 (2017) 103–124.
[3] J. Jirousek, P. Teodorescu, Large finite elements method for the solution of problems in the theory of elasticity, Comput. Struct. 15 (1982) 575–587.
[4] J. Jirousek, P. Teodorescu, Hybrid-Trefftz plate bending elements with p-method capabilities, Int. J. Numer. Methods Eng. 24 (1987) 1367–1393.
[5] E. Kita, N. Kamiya, Trefftz method: an overview, Adv. Eng. Softw. 24 (1995) 3–12.
[6] D.S. Zézé, M. Potier-Ferry, N. Damil, A boundary meshless method with shape functions computed from the PDE, Eng. Anal. Bound. Elem. 34 (8) (2010) 747–754.
[7] J. Yang, H. Hu, Y. Koutsawa, M. Potier-Ferry, Taylor meshless method for solving non-linear partial differential equations, J. Comput. Phys. 348 (2017) 385–400.
[8] Y. Tampango, M. Potier-Ferry, Y. Koutsawa, S. Tiem, Coupling of polynomial approximations with application to a boundary meshless method, Int. J. Numer. Methods Eng. 95 (13) (2013) 1094–1112.
[9] H. Liebowitz, E.T. Moyer, Finite element methods in fracture mechanics, Comput. Struct. 31 (1989) 1–9.
[10] T. Belytschko, R. Gracie, G. Ventura, A review of extended/generalized finite element methods for material modeling, Model. Simul. Mater. Sci. Eng. 17 (2009) 043001.
[11] W.K. Wilson, Combined Mode Fracture Mechanics, Ph.D. thesis, University of Pittsburgh, 1969.
[12] D.M. Tracey, Finite elements for determination of crack tip elastic stress intensity factors, Eng. Fract. Mech. 8 (1971) 255–265.
[13] S.E. Benzley, Representation of singularities with isoparametric finite elements, Int. J. Numer. Methods Eng. 8 (1974) 131–150.
[14] J.M. Melenk, I. Babuška, The partition of unity finite element method: basic theory and applications, Comput. Methods Appl. Math. 139 (1996) 289–314.
[15] N. Moës, J. Dolbow, T. Belytschko, A finite element method for crack growth without remeshing, Int. J. Numer. Methods Eng. 46 (1999) 131–150.
[16] Z.C. Li, Combined Methods for Elliptic Equations with Singularities, Interfaces and Infinities, Kluwer Academic Publishers, Dordrecht, 1998.
[17] Z.C. Li, T.T. Lu, H.T. Huang, A.H.D. Cheng, Trefftz, collocation, and other boundary methods: a comparison, Numer. Methods Partial Differ. Equ. 23 (2007) 93–144.
[18] G. Fairweather, A. Karageorghis, The method of fundamental solutions for elliptic boundary value problems, Adv. Comput. Math. 9 (1–2) (1998) 69–95.
[19] X. Zhang, X.H. Liu, K.Z. Song, M.W. Lu, Least-squares collocation meshless method, Int. J. Numer. Methods Eng. 51 (9) (2001) 1089–1100.
[20] P. Grisvard, Elliptic Problems in Nonsmooth Domains, Pitman, Marshfield, 1985.
[21] M. Dauge, Elliptic Boundary Value Problems on Corner Domains: Smoothness and Asymptotics of Solutions, Springer, Berlin, Heidelberg, 1988.
[22] F. Hecht, New development in FreeFem++, J. Numer. Math. 20 (3) (2012) 251–265.
[23] M. Costabel, M. Dauge, Z. Yosibash, A quasi-dual function method for extracting edge stress intensity functions, SIAM J. Math. Anal. 35 (2004) 1177–1202.
[24] J.M. Muller, N. Brisebarre, F. de Dinechin, C.-P. Jeannerod, V. Lefèvre, G. Melquiond, N. Revol, D. Stehlé, S. Torres, Handbook of Floating-Point Arithmetic, Springer, Dordrecht, 2010.
[25] E.J. Kansa, P. Holoborodko, On the ill-conditioned nature of C^{∞} RBF strong collocation, Eng. Anal. Bound. Elem. 78 (2017) 26–30.
[26] G.C. Sih, On the Westergaard method of crack analysis, Int. J. Fract. 2 (4) (1966) 628–631.
[27] N.I. Muskhelishvili, Some Basic Problems of the Mathematical Theory of Elasticity, Springer Netherlands, 1977.